

# State-of-the-art Noncontact Gauge Meter for Flat Rolling and Cold-rolled Precision Metals Expected for Microsensor Application

Yoshihiro Hosoya,<sup>1\*</sup> Elke Roller,<sup>2</sup> Hiroyuki Yoshimi,<sup>1</sup> Kohsuke Endou,<sup>1</sup>  
Kazuma Takahashi,<sup>1</sup> Yuta Matsumura,<sup>1</sup> and Shuhei Hiruta<sup>1</sup>

<sup>1</sup>Tokushu Kinzoku Excel, Co., Ltd. 56, Tamagawa, Tokigawa-machi, Saitama 355-0342, Japan

<sup>2</sup>Friedrich Vollmer Feinmessgeratebau GmbH, Germany  
Verbandsstrasse 60b, D-58093 Hagen, Germany

(Received December 20, 2018; accepted April 4, 2019)

**Keywords:** cold rolling, sensor material, noncontact gauge meter, clad metal, resistor materials, spring materials, medical materials, diaphragm pump

In this paper, by focusing on cold-rolled precision metals widely used as sensor materials, a state-of-the-art noncontact gauge meter, which enables high-precision thickness control in a cold-rolling mill with high thickness tolerance, is introduced as a sensor technology, and the following three typical precision thin gauge metals, which are expected as the reverse use of the sensor technology, are introduced as the material technology: (1) clad metal used for electronic sensors, (2) ultrahigh-strength thin gauge stainless steel with high durability for haptic device applications, and (3) ultrafine grain metal foil to be applied to a medical diaphragm micropump.

## 1. Introduction

With recent progress in both computer and sensor technologies, the manufacturing facilities based on craftsmanship that once relied on human eyes and intuition have been replaced by advanced automatic process controlling technologies of today. The sensor instantaneously detects both the various dimensions and physical quantities of products as an eye or tactile sense of the manufacturing apparatus, and the data detected by sensors are converted into electronic signals, which are provided to the process computer. Various physical quantities, such as electrical, magnetic, optical, thermal, and mechanical ones that are peculiar to metals, have been utilized for sensor tips.<sup>(1)</sup> In contrast to the above use of sensors, the sensor technology is also applied to various devices that generate perceptive and haptic signals.

As the principle of gauge control during rolling, Figs. 1 and 2 show the schematic diagrams with the controlling factors of rolling and the logic of dynamic control for roll gap, respectively. To reduce the thickness of a strip from an initial thickness ( $h_1$ ) to a target thickness ( $h_2$ ), the curve of rolling force as a function of the plastic deformation of the strip ( $N$ ) and the mill constant line ( $M$ ) are used to preset an initial roll gap ( $S_0$ ). Since curve  $N$  varies with the friction coefficient ( $\mu$ ), strip tension ( $t$ ), rolling velocity ( $v$ ), and so forth,  $h_2$  is kept constant by

---

\*Corresponding author: e-mail: y-hosoya@tokkin.co.jp  
<https://doi.org/10.18494/SAM.2019.2245>

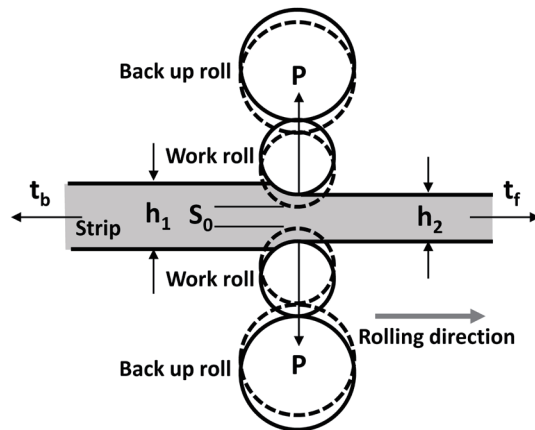


Fig. 1. Schematic diagram of rolling and its controlling factors.

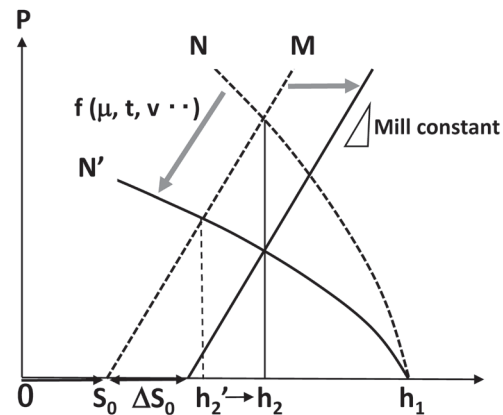


Fig. 2. Principle of thickness control in rolling.

shifting  $S_0$  to  $(S_0 + \Delta S_0)$  when curve  $N$  changes to curve  $N'$ . Furthermore, since the scattering of  $h_1$  is inevitable in a real strip, it is essential to accurately detect the strip thickness before and after rolling with high response for the dynamic control of rolling.

Regarding the dynamic controlling system of strip thickness, the gauge meter automatic gauge control (AGC) called BISRA AGC has been a basic tool for AGC thus far. Besides the progress in thickness control systems, many subsequent developments for the crown and shape controlling systems have been established<sup>(2)</sup> to meet the growing demands for flat-rolled precision metals with as small tolerance as possible. However, the most important devices in these systems are still gauge sensors. In a single stand rolling mill, two gauge sensors are installed at both sides of the rolling mill, and the thickness data detected by gauge meters are provided to the AGC system and simultaneously displayed on the monitor for operation.

## 2. Development of State-of-the-art Noncontact Gauge Meter for Flat Rolling

For the measurement of strip thickness, either a noncontact measurement method using an X-ray or gamma ray sensor or a contact measurement method using a flying contact gauge has been commonly employed. The noncontact method is an indirect method of estimating the strip thickness by calibration with a reference metal piece with the correction of the absorption of radiation, whereas the contact method is a direct method of measuring the strip thickness by cramping by sensor tips and evaluating the deviation from the thickness of the calibration sample. As to a single-stand reversing mill, the latter method has been used worldwide, but either the contact marks on the strip by diamond tips or the adhesive reaction between the diamond tips and the strip such as titanium has been an unsolved problem.

To solve these problems, a noncontact gauge meter using blue laser light was developed by Vollmer GmbH in Germany.<sup>(3,4)</sup> Figure 3<sup>(4)</sup> shows both the contact gauge meter (VBM) and the noncontact gauge meter (VTLG) developed by Vollmer GmbH. The VTLG was developed with the following concepts to compensate for the drawbacks of the VBM and other noncontact gauge meters by using an X-ray or gamma ray sensor:

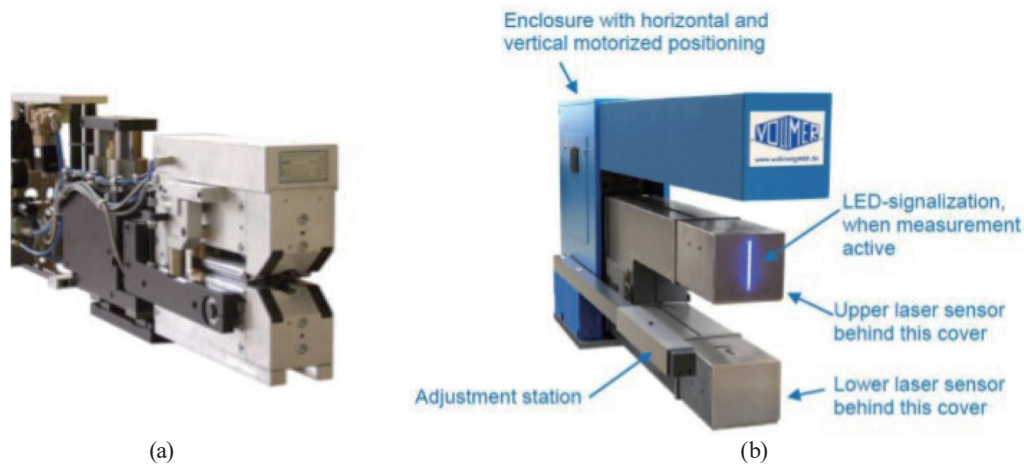


Fig. 3. (Color online) Two types of gauge meter developed by Vollmer GmbH.<sup>(4)</sup> (a) Contact gauge meter (VBM) and (b) noncontact gauge meter (VTLG).

- (1) contact-free and fully automatic,
- (2) absolute thickness measurement irrespective of the alloy contents, and
- (3) minimum maintenance and high cost-performance ratio.

The major specifications and features of three types of gauge meter, i.e., X-ray/gamma ray, VTLG, and VBM, are summarized in Table 1. The VTLG consists of a C-frame fitted with laser sensors at its tips. The C-frame moves towards the width direction of the strip in order to measure the thickness profile of the 680 mm<sup>w</sup> whole strip as shown in Fig. 4.<sup>(4)</sup> The green line shows the thickness deviation from the target thickness of 1440  $\mu\text{m}$  at the different width positions. The good resolution is a result from the small measurement spot diameter of the VTLG and the high measurement frequency.

Since the laser sensors are optical systems, not only rolling mills but also a wide range of applications can be expected. For example, they are applicable to slitting, recoiling, and leveling lines.

The key development in the VTLG is the application of laser sensors. The basic technology applied to the VTLG is laser triangulation. The system operates with a wavelength of 405 nm at a power of 15 mW, i.e., blue laser. The diameter of the measurement spot is only 0.1 mm. Since the signal has an extremely low noise and a very short exposure time, the laser sensors achieve extremely high definition images and are further enhanced by using multilens focusing optics. The VTLG applies a very small and extremely focused laser beam, which enables us to see not only one reflection point on the strip surface but also another point, namely, the point on the strip itself and a point on the surface of the moisture (oil or emulsion). The VTLG distinguishes between these two images and of course uses the image from the strip surface for the measurement. Therefore, it is possible to measure only the strip thickness with the VTLG despite the presence of oil or emulsion on the strip surface and to avoid measurement errors due to the oil or emulsion layer.

Regarding the laser control system, the VTLG operates with a measuring frequency of up to 80 kHz in the upper C-frame arm and in the lower C-frame arm, independently. The

Table 1

Comparison of the major specifications and features of VTLG, VBM, and radiation methods by X-ray or gamma ray.

Noncontact type		Contact type
X-ray/gamma ray	VTLG	VBM
Thickness measurement related to exact knowledge and perfect compensation of alloy composition	Measurement direct and absolute	Measurement direct and absolute but depending on good alignment and calibration of the gauge
Noncontact, means no marking risk on the strip and chance for installing protection device against damage by strip breakages	Noncontact, means no marking risk on the strip and chance for installing protection device against damage by strip breakages	Contact. Risk for strip marking and no protection against damage by strip breakages possible (but already included break pins to keep possible damage small)
Dangerous Radiation. Protection of operators needed	No operator protection needed	No operator protection needed
Governmental permission for use needed	No permission needed	No permission needed
In case of gamma ray: Radioactive material is inside. Radioactive waste management needed	Not relevant	Not relevant
Wrong measurement can be noticed only in a following line or after customer complaint	Self controlled: Automatic self-test for correct measurement	Wrong measurement can be noticed only in a following line or after customer complaint
Cross profile measurement possible	Cross profile measurement possible	No cross profile measurement possible
Measurement spot diameter 20–40 mm	Measurement spot diameter 0.1 mm	Measurement spot diameter 1 mm

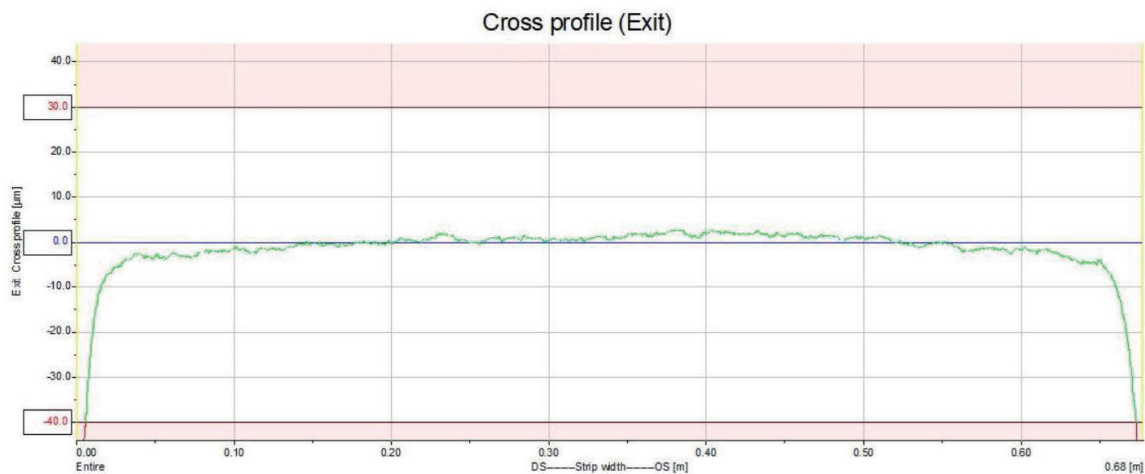


Fig. 4. (Color online) Typical thickness profile of the width of whole strip measured by the VTLG.<sup>(4)</sup>

laser controller has to synchronize the individual measurements of the two sensors to the microsecond; otherwise, any vibration of the strip would result in a measurement error.

Figure 5 shows the VTLG installed in the No. 3 Z-Hi cold-rolling mill newly operated in the beginning of 2019 at the Taiwan Facility of Tokushu Kinzoku Excel Co., Ltd. The expected performance of the VTLG has been obtained from the beginning of operation.

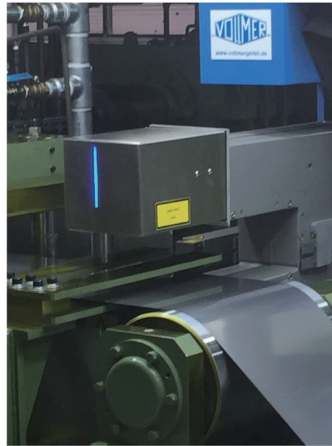


Fig. 5. (Color online) VTLG installed in the No. 3 Z-Hi cold-rolling mill newly operated in the beginning of 2019 at the Taiwan Facility of Tokushu Kinzoku Excel Co., Ltd.

### 3. Typical Precision Metals Expected for Microsensor Application

As the reverse use of the sensor technologies in manufacturing, the following three typical flat-rolled thin gauge metals expected as the sensor materials manufactured by Tokushu Kinzoku Excel Co., Ltd. are introduced below.

#### 3.1 Clad metals used as electronic sensors

By cladding the metals with different physical and mechanical properties, it is possible to produce composite materials with various multiple functions depending on the kind of metal and the number of layers. A bimetal material, in which two kinds of metal with different coefficients of thermal expansion (CTEs) were laminated, has been widely used as a thermal sensor.

Table 2 shows the typical composition of clad metals and their applications. In the case of two-layer cladding, the hybridization of nonferrous metals with different electrical and thermal properties is mainstream, but in the case of multilayer cladding, stainless steel is used as a core metal to hybridize its strength with the physical properties of nonferrous metals such as electric and thermal conductivities. Stainless steel has also been expected as an anticorrosion metal.

Then, we introduce a typical sensor application of a clad metal, that is, the shunt resistor chip. Recently, from the conventional application of the shunt for detecting the analog current shown in Fig. 6(a), the clad material for the shunt resistor for controlling the current of automobiles and telecommunication equipment shown in Fig. 6(b) has become mainstream.

Figure 7 shows a schematic diagram of a cross-sectional structure of a shunt resistor to be mounted on an IC board. The main part is a two-layer clad of resistor alloy and copper (Cu), which serves as a lead wire; furthermore, a soldering layer is provided to one side to be mounted on the IC board and a black insulating coating layer to the opposite side. Both the core technologies and the technological solutions are summarized in the figure. The most important

Table 2  
Typical composition of clad metals and their applications.

Types of clad	Constitution of clad	Hybridization of properties	Typical applications
Multilayered clad	Noble metal/Cu	High electric conductivity	Electrical connectors
	Noble metal/Cu alloy	High corrosion resistance	
	Ni/KOV	Low thermal expansion High corrosion resistance	PGA caps
Triple-layered clad	Cu/SUS	High strength	Springs for relay device
	Cu/Fe	High electric conductivity	
	Cu/KOV	Low thermal expansion	Disk diode
	Cu/INVAR	High electric conductivity	
	CN/PC	Stabilization of magnetic properties	
Double-layered clad	Ni/SUS	High corrosion resistance	Electrical connectors
	Cu/Al	Weight reduction High corrosion resistance	Heat sink
	Fe/Cu	Heat dissipation	Heat spreader
	SUS/Cu	High strength	
	Al/SUS	High strength Weight reduction	Enclosure of electric device

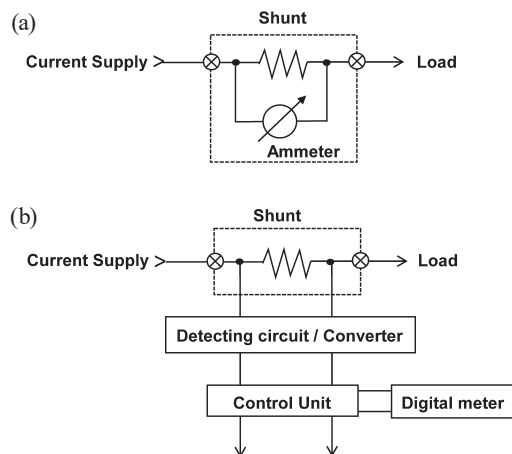


Fig. 6. Recent progress in the application of shunt resistor as a sensor for state-of-the-art devices. (a) Conventional application of shunt resistor for expansion of measuring range of ammeter. (b) Recent sensor application for the IC current detection composed of shunt resistor.

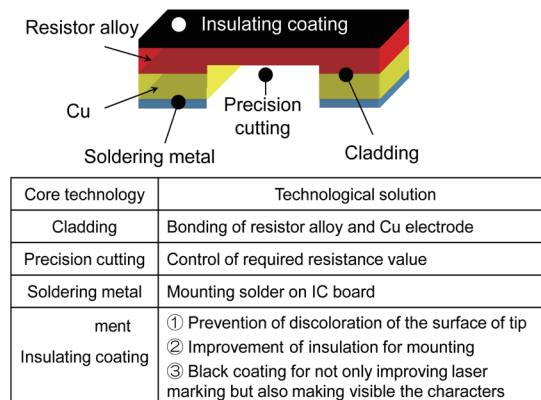


Fig. 7. (Color online) Structure of current-detecting shunt resistor tip for mounting IC board.

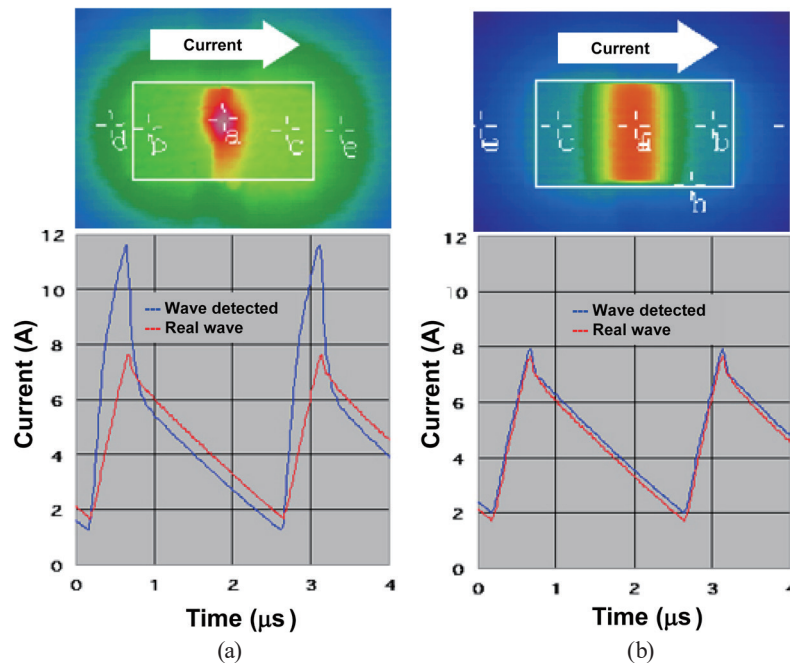


Fig. 8. (Color online) Comparison between conventional and state-of-the-art resistors.<sup>(5)</sup> (a) Conventional resistor whole resistivity was adjusted by trimming at side edge and (b) improved resistor whose resistivity was adjusted by precision cutting on plate surface.

feature of this type of resistor chip is that the resistivity is precisely tuned by precisely cutting one side of the resistor material, in comparison with a conventional resistor whose resistivity is tuned by trimming the side edge of the chip.

Figure 8<sup>(5)</sup> shows the comparison of the basic characteristics of resistors between the type shown in Fig. 7 and the conventional type. Although the heat generation of the resistors is not uniform and the overcurrent due to the inductance of the resistors is observed in the conventional type, the generated heat distributes uniformly, and the same current wave, as well as the source current wave, is detected in the type shown in Fig. 7.

### 3.2 High-strength thin gauge metal for highly reliable metallic lateral vibration devices

Metallic materials used for smartphones occupy large parts such as bodies, reinforcements, electric contact parts, and vibrating parts for haptic devices. In particular, in the example of the vibration motor shown in Fig. 9,<sup>(6)</sup> reliable stainless steel leaf springs bent as hairpin-shaped structures are installed in the device as a lateral vibration motor; therefore, the following performance is required on the material itself:

- (1) high accuracy of a material's thickness that dominates spring performance,
- (2) excellent bendability and less scattering of bending radius,
- (3) sufficient weldability to attach to a device,
- (4) sufficient fatigue life and high fatigue limit to the number of cycles of  $10^8$ ,
- (5) sufficient impact fracture toughness in case of dropping, and
- (6) sufficient corrosion resistance in the circumstances for use.

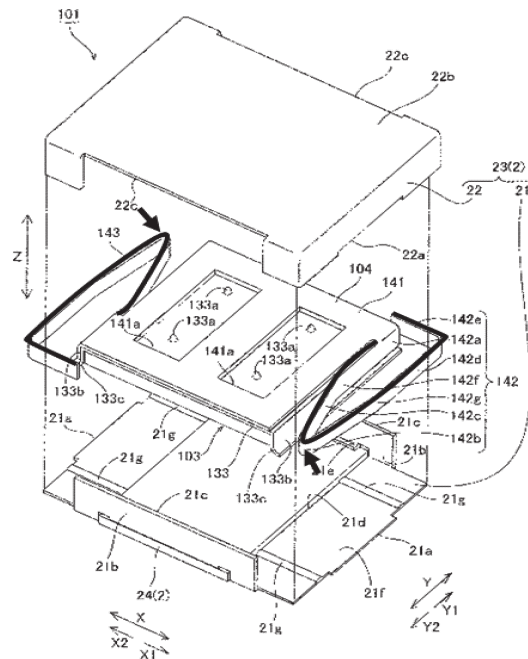


Fig. 9. Typical construction of the lateral vibration motor.<sup>(6)</sup>

From the viewpoint of material design, we developed the material based on the following concepts.

- (1) Alloy design is based on commercial stainless steel.
- (2) The microstructure is controlled under near equilibrium condition.
- (3) To maintain both high yield strength and high flow stress, the stress-strain curve is controlled to the ideal elastoplastic deformation.
- (4) To realize high yield strength, strain-induced martensite ( $\alpha'$ ) additionally precipitation-hardened is considered for the matrix.
- (5) The microstructure in which the  $\alpha'$ -phase surrounds the retained austenite phase ( $\gamma$ ) is considered the target microstructure.
- (6) In the plastic deformation process, the hardness difference between the metastable  $\gamma$ -phase and the  $\alpha'$ -phase decreases owing to the strain-induced transformation of the  $\gamma$ -phase to the  $\alpha'$ -phase, and the volume expansion due to the  $\gamma \rightarrow \alpha'$  transformation compresses the generation of microcracks.
- (7) In the  $\gamma$ -phase, fatigue resistance is improved by considering the crack propagation resistance due to  $\alpha'$ -transformation in the plastic region of the crack tip and stopping the crack propagation by the network structure of the  $\alpha'$ -phase.

The strength and ductility balance of the developed material, which has been in mass production, are shown in Fig. 10.<sup>(6)</sup> In addition to having an excellent strength-ductility balance superior to conventional high-strength steel sheets, the scattering of the developed material is also very small. As shown by the typical stress-strain curves in Fig. 11,<sup>(6)</sup> both ideal elastoplastic deformation curves and a very small planar anisotropy are obtained.



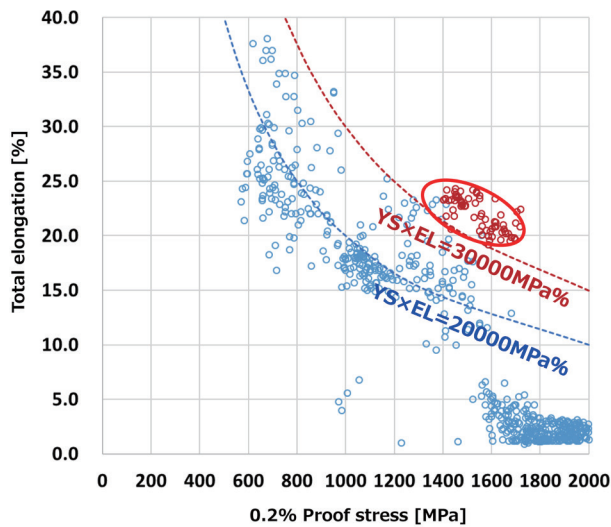


Fig. 10. (Color online) Strength and ductility balance of the developed material that has already been mass-produced.<sup>(6)</sup>

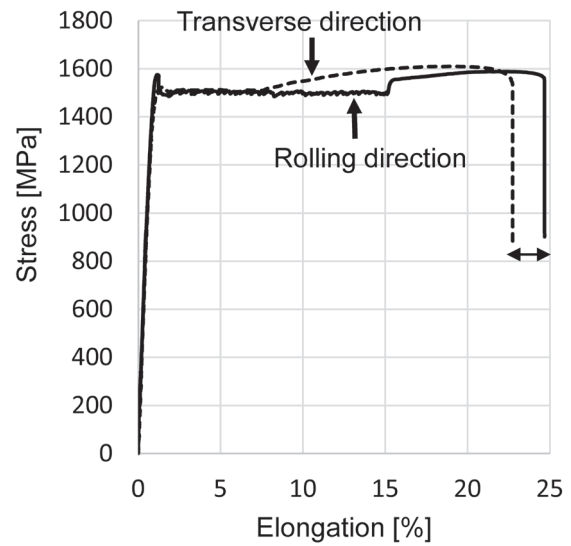


Fig. 11. Typical stress-strain curves in both rolling and transverse directions of the developed steel.<sup>(6)</sup>

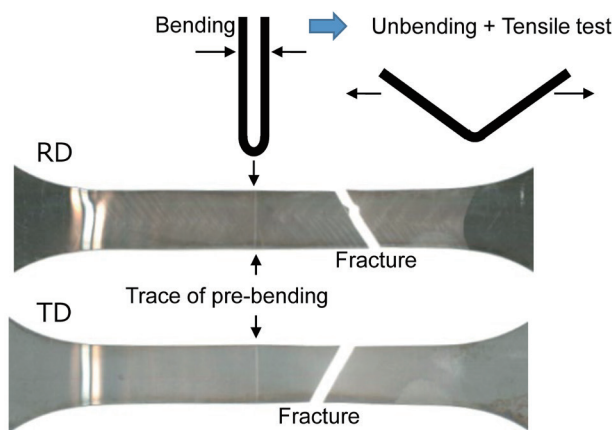


Fig. 12. (Color online) Results of evaluating an anti-secondary work embrittlement due to hairpin bending in different directions.<sup>(6)</sup> (RD: rolling direction, TD: transverse direction)

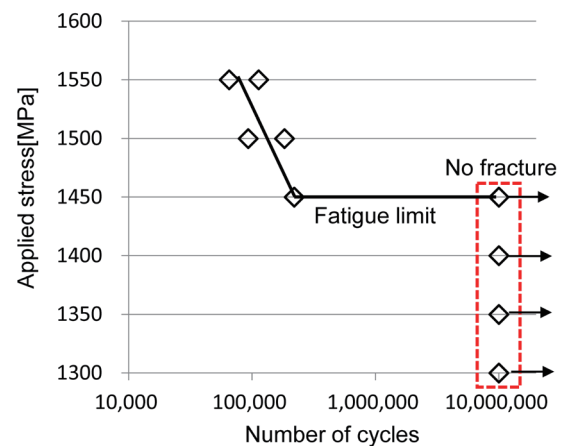


Fig. 13. (Color online) Result of the tension-tension fatigue test on the developed steel.<sup>(6)</sup>

The results of evaluating an anti-secondary work embrittlement after hairpin bending are shown in Fig. 12.<sup>(6)</sup> By bending close to the contact followed by unbending plus tensile testing, the sample was confirmed to be broken at the portion other than the bent portion regardless of the bending direction. Furthermore, the result of the tension-tension fatigue test shown in Fig. 13<sup>(6)</sup> revealed that the developed material had an extremely high fatigue limit of 1450 MPa, demonstrating excellent reliability and durability. Consequently, the developed material is not limited to being applied to vibration motors of haptic devices, but is expected to be widely applied as the sensor material.

### 3.3 Multilayered metallic micropump as a liquid flow control device

As a final example, we introduce a metal micropump as a compact and wearable infusion pump that replaces the intravenous injection system. The diaphragm pump that directly infuses through the reciprocating motion of a piezoelectric disc (PZT) can reduce the dead volume of the pump in comparison with other centrifugal and piezoelectric vibration pumps; thus, it can be downsized to the size on the fingertip.<sup>(7)</sup> In addition to this, high-precision flow rate control is possible using an electronic control unit as a reverse application of the sensor technology.

The external appearance and sectional structure of the diaphragm pump are shown in Fig. 14.<sup>(7)</sup> Compared with the other metal micropump produced from titanium alloy,<sup>(8)</sup> the pump body has a structure in which eight stainless steel sheets and foils are laminated, and stainless steel foils of 10  $\mu\text{m}$  thickness are laminated at the driving part. To obtain stable pumping performance, it is effective to control the microstructure of the stainless steel foil to have both uniform and fine grains, which improves not only the processing accuracy of the edge quality of flow holes but also the uniform bonding interface as shown in Fig. 15.<sup>(7)</sup>

To obtain a fine grain structure, cold rolling and  $\alpha' \rightarrow \gamma$  reverse transformation are repeated. The thin gauge stainless steel with a fine grain structure has excellent characteristics in terms of not only the diffusion bonding property but also the product surface quality. Figure 16 shows the effect of grain size on the outer surface after U-bending in the stainless steels with average grain sizes of (a) 10 and (b) 1  $\mu\text{m}$ . The test conditions used are a sheet thickness of 100  $\mu\text{m}$  and a bending radius of 90  $\mu\text{m}$ . An extremely smooth surface can be obtained by refining the grain size. Such a smooth surface can be considered to have superior performance for a mechanical sensor, which is required to obtain durability and reliability.

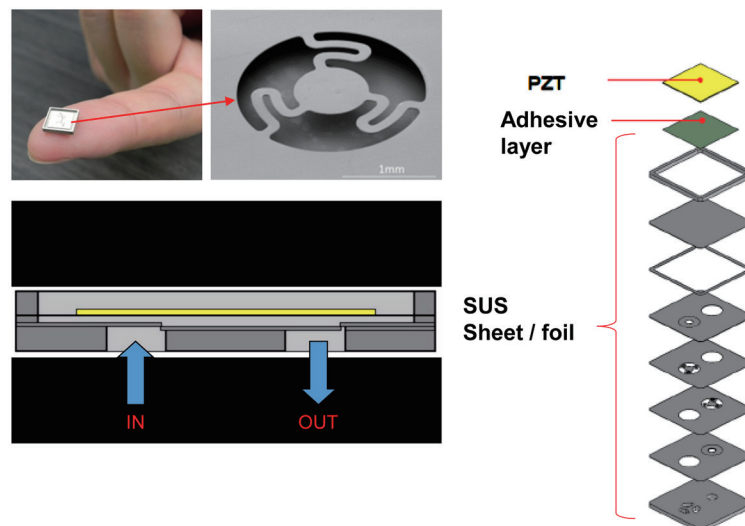


Fig. 14. (Color online) External appearance and sectional structure of the diaphragm pump made of thin gauge stainless steel with fine grain structure.<sup>(7)</sup>

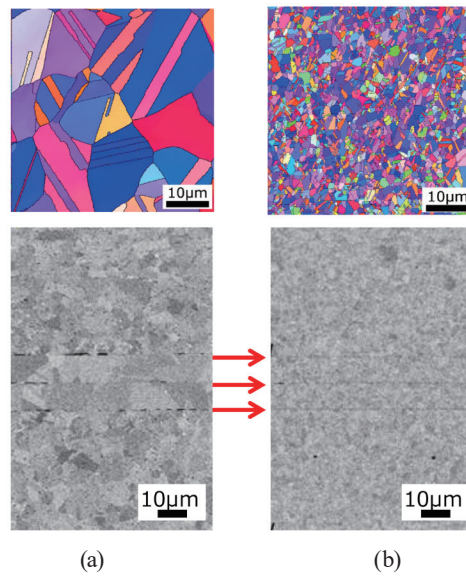


Fig. 15. (Color online) Effect of the grain size on the diffusion bonding interface diaphragm pump.<sup>(7)</sup> Mean grain diameters of (a) and (b) are 10 and 1  $\mu\text{m}$ , respectively.

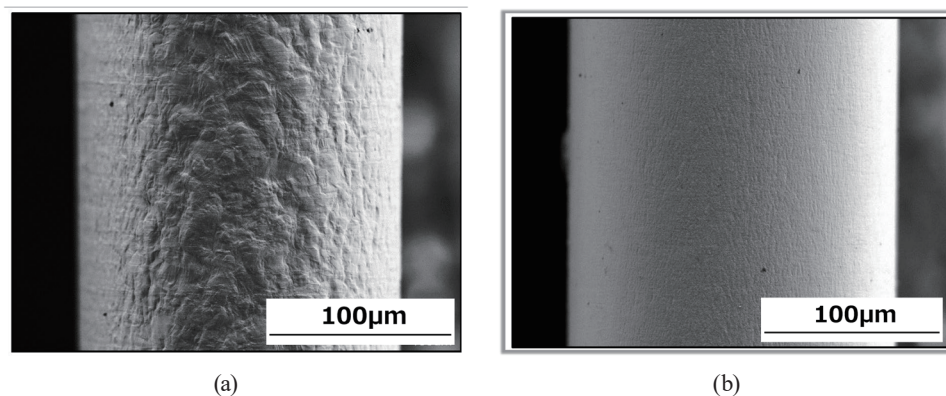


Fig. 16. Effect of grain size on the outer surface after U-bending in the stainless steels with average grain sizes of (a) 10 and (b) 1  $\mu\text{m}$ . Test conditions: sheet thickness of 100  $\mu\text{m}$  and bending radius of 90  $\mu\text{m}$ .

#### 4. Conclusion

It is not too much to say that the recent progress in sensor technologies has been brought by not only information technologies and computer-aided process controlling technologies, but also the innovation of sensing materials. In this paper, by focusing on the cold rolling of precision metals, examples of innovations on both cold-rolling technology and cold-rolled materials were introduced using the core businesses of Vollmer GmbH and Tokushu Kinzoku Excel Co., Ltd.

In recent years, the VTLG has steadily been introduced to cold-rolling manufacturers around the world by recognizing its advantage for both high performance as gauge sensor and wide range application for various materials. On the other hand, precision cold-rolled metals with a fine grain structure are not only used for various electronic devices but also expected to expand their use as various sensor materials.

### References

- 1 K. Goto: *Trans. JIM* **23** (1984) 978.
- 2 F. Fujita and S. Yamaguchi: *Tetsu-to-Hagane* **100** (2014) 2 (in Japanese).
- 3 E. Roller: *MPT Int.* **6** (2016) 42.
- 4 E. Roller: IWCC Technical Seminar (2018, Chicago) 1–12.
- 5 KOA CORPORATION: <https://www.koaglobal.com/product/shunt> (accessed October 2019).
- 6 Y. Matsumura, K. Ogawa, Y. Hosoya, S. Tanaka, M. Shimasaki, and T. Hirata: *Mater. Jpn.* **57** (2018) 20.
- 7 Nagano Prefecture Techno Foundation: Final Report entitle “Development of processing technology for nano-precision micro parts using SUS 304 superplasticity” (2016) supported by the Supporting Project for Advancement of Strategic Basic Technology 2015.
- 8 W. W. Wits, S. J. Weitkamp, and J. van Es: *Procedia CIRP* **7** (2013) 252.